

# Water-Assisted Growth of Aligned Carbon Nanotube–ZnO Heterojunction Arrays\*\*

By Jianwei Liu, Xiaojun Li, and Liming Dai\*

1D heterojunction structures based on nanomaterials are of significance to both scientific fundamentals in nanoscience<sup>[1]</sup> and potential applications in nanoscale systems, including various new electronic and photonic nanodevices.<sup>[2,3]</sup> Consequently, considerable effort has been made in recent years to devise and characterize various heterojunctions between different low-dimensional nanomaterials.<sup>[4]</sup> Examples include the syntheses of doped GaN-based core/shell/shell (n-GaN/In-GaN/p-GaN) nanowire heterostructures through metal-organic chemical vapor deposition (MOCVD),<sup>[5]</sup> aligned ZnO heterojunction arrays on GaN, Al<sub>0.5</sub>Ga<sub>0.5</sub>N, and AlN substrates by a vapor–liquid–solid phase process using gold as a catalyst,<sup>[6]</sup> multiwalled CNT–zinc sulfide (CNT: carbon nanotube) heterojunctions by a combination of ultrasonic and heat treatments,<sup>[7]</sup> CNT–silicon nanowire heterojunctions by localizing a suitable metal catalyst at the end of a preformed nanotube or nanowire,<sup>[2a]</sup> and SWNT–gold (SWNT: single-walled carbon nanotube) nanorod heterojunctions through the selective solution growth of Au nanorods on an SWNT structure.<sup>[8]</sup> Among them, CNT-based 1D heterojunctions are of particular interest because of the unique molecular geometry as well as excellent electronic, thermal, and mechanical properties intrinsically associated with CNTs.<sup>[9]</sup>

On the other hand, ZnO nanostructures are shown to possess superior optoelectronic properties useful in nanoscale transistors,<sup>[10]</sup> sensors,<sup>[11]</sup> electron emitters,<sup>[12a]</sup> and many other systems.<sup>[12b–d]</sup> The large-scale formation of heterojunctions of ZnO with other nanomaterials (particularly CNTs) should extend the scope of ZnO nanomaterials for potential applications. Although recent work has demonstrated the large-scale growth of aligned ZnO nanowire arrays,<sup>[13]</sup> the formation of large-area ordered heterojunctions of ZnO nanostructures with other semiconducting materials has been much less discussed in the literature.<sup>[6]</sup> In particular, the growth of aligned CNT–ZnO heterojunction arrays remains a big challenge. Here, we report the first synthesis of large-scale aligned CNT–ZnO heterojunctions simply by water-assisted chemical

vapor deposition (WACVD) of carbon on a zinc foil, which acts as both the substrate for the CNT growth and zinc source for the formation of the ZnO nanostructures. Water, as a weak oxidizer, provides the oxygen source for the formation of ZnO nanostructures and also enhances CNT growth.<sup>[14]</sup> This cost-effective and efficient approach requires no other catalytic reagent and allows the large-scale formation of heterojunctions between the perpendicularly aligned CNTs and ZnO nanostructures through a natural contact. As we shall see later, the intimately connected heterojunctions between the aligned CNTs and ZnO nanostructures thus prepared possess interesting optoelectronic properties attractive for many potential applications, including their use as electro-optic sensors and field emitters.

Briefly, the formation of the aligned CNT and ZnO heterojunctions was achieved by carrying out pyrolysis of C<sub>2</sub>H<sub>2</sub> on a zinc foil supported by a quartz glass plate in a tube furnace at 850 °C under a combined flow of Ar and H<sub>2</sub>, with a portion of the carrier gas passing through a water bubbler, followed by annealing with a flow of Ar via the water bubbler passing through the reaction system. Figure 1a shows a low-magnification scanning electron microscopy (SEM) image of the as-synthesized CNT–ZnO sample, revealing a large-scale aligned array. Although the corresponding SEM images under higher magnification in Figure 1b and c show some misalignment at the top of the nanotube array, Figure 1b clearly shows the CNT–ZnO heterojunction with a ZnO crystal (bright spot) attached on the tip of each of the constituent aligned CNTs. Figure 1c further reveals that approximately 40 % of the ZnO nanoparticles are of hexagonal morphology. The corresponding transmission electron microscopy (TEM) image in Figure 1d shows that the CNT thus prepared is multiwalled, and that the ZnO nanoparticle is intimately connected to the aligned CNT structure. The multiwalled CNT with an inner diameter of approximately 30 nm and outer diameter of approximately 60 nm possesses a bamboolike structured hollow core, similar to those prepared by solvothermal reduction of ethanol in the presence of Mg<sup>[15]</sup> or pyrolysis of FePc.<sup>[16]</sup> Figure 1e shows the selected-area electron diffraction (SAED) pattern of the ZnO nanoparticle, which indicates that the as-prepared ZnO nanoparticle is single crystalline and can be indexed as hexagonal wurtzite ZnO.<sup>[17]</sup> The aligned CNT–ZnO heterojunctions thus prepared were further investigated using energy-dispersive X-ray spectroscopy (EDS) in a scanning electron microscope. As expected, the line-scanning EDS profiles for Zn and C clearly show a dramatic decrease in the Zn (and corresponding increase in C) content along the scanning

[\*] Prof. L. Dai, Dr. J. Liu, Dr. X. Li  
Department of Chemical and Materials Engineering  
School of Engineering, University of Dayton  
300 College Park, Dayton, OH 45469-0240 (USA)  
E-mail: ldai@udayton.edu

[\*\*] This work was supported by the NSF (CCF-0403130), ACS (PRF 39060-ACSM), AFOSR, AFRL/ML, Wright Brothers Institute, Dayton Development Collation, and the University of Dayton. We acknowledge the NEST Lab at UD for the access of SEM and TEM facilities.

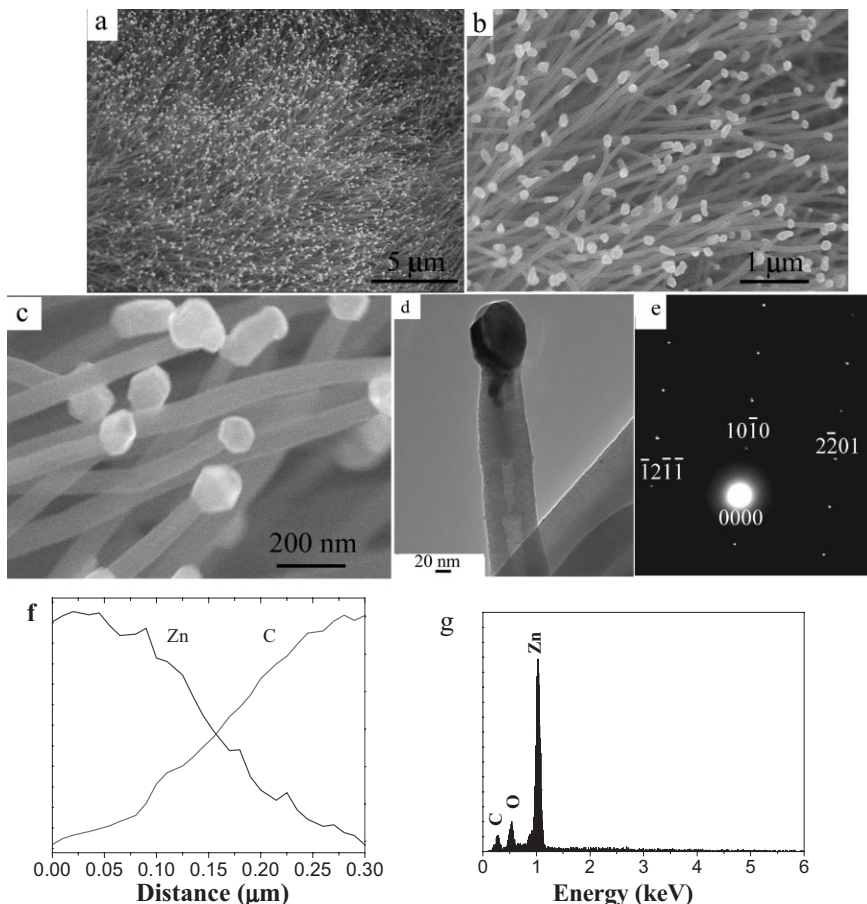


**Figure 1.** a) Low-magnification SEM image of an aligned CNT–ZnO heterojunction array. b,c) As for (a), under higher magnification. d) Transmission electron microscopy (TEM) image of a typical CNT–ZnO heterojunction and a selected-area electron diffraction (SAED) pattern of a ZnO tip (e). f) Energy-dispersive X-ray spectroscopy (EDS) line-scanning profile of CNT–ZnO heterojunctions from the ZnO tip to the CNT. g) A point-focused EDS profile on the ZnO tip.

path from the ZnO tip to the CNT (Fig. 1f). The point-focused EDS profile from the ZnO tip shows intense Zn and O peaks with a much smaller C peak (Fig. 1g). The co-existence of Zn and C peaks in the point-focused EDS profile from the tip indicates, most probably, that the nanotube adopted a “tip-growth” mechanism<sup>[18]</sup> with the Zn catalyst forming in the initial stage of the growth process moving up along the growing nanotube. Subsequent annealing under the mixed flow of Ar and water further facilitated the growth of the ZnO tips. Indeed, we observed that a prolonged post-synthesis annealing under the mixed flow caused a significant increase in the size of the ZnO tip (see below), and that only metal nanoparticles smaller than the tube diameter were formed at the tips of the aligned CNTs prepared without the post-synthesis annealing, as shown in Figure 2a. During the annealing process, therefore, water might

have “etched” the nanotube top cap to expose the Zn catalyst particle for the formation of ZnO and further growth. By eliminating water from the reaction system, we did not produce any aligned CNTs (Fig. 2b), confirming the role of water in enhancing aligned CNT growth in this particular case. It has been recently reported that the addition of an appropriate amount of water vapor during the growth of aligned CNTs can effectively oxidize the amorphous carbon coating, if any, on catalyst particles, leading to enhanced catalytic activity and a longer lifetime.<sup>[14]</sup>

Further details of the formation of the CNT–ZnO heterojunction were obtained from X-ray photoelectron spectroscopic (XPS) studies. Figure 3a represents an XPS survey spectrum of an as-prepared sample, which shows the presence of C, O, and Zn with the O/Zn ratio calculated to be 1.15—a value that varied little with excessive heating (ca. 500 °C) and/or pumping (ca. 10<sup>−7</sup> Torr; 1 Torr ≈ 133 Pa) for a prolonged time. Given possible errors associated with the atomic-ratio calculation from an XPS survey spectrum, the value of 1.15 is consistent with the corresponding O/Zn ratio of 1 calculated from the molecular structure of ZnO. This indicates that any possible oxygen adsorption from air onto the nanotube surface<sup>[19]</sup> is negligible in this particular case. The high-resolution XPS spectra

of Zn 2p<sub>3/2</sub>, O 1s, and C 1s are shown in Figure 3b–d, respectively. The strong peak at 1022 eV seen in Figure 3b can be attributed to Zn<sup>2+</sup>. The O 1s peak at 530.6 eV is attributable to O<sup>2−</sup> in the ZnO crystal lattice, a typical value for zinc oxide networks.<sup>[20]</sup> The high-resolution XPS C 1s peak at 284.4 eV,

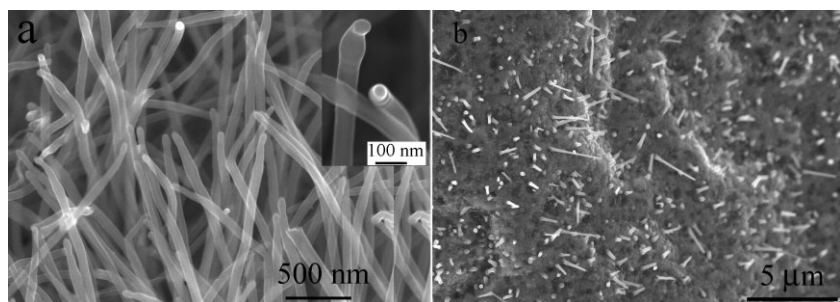


**Figure 2.** a) SEM image of an as-prepared sample without the post-synthesis annealing. b) SEM image of an as-prepared sample without the introduction of water vapor into the nanotube growth atmosphere.

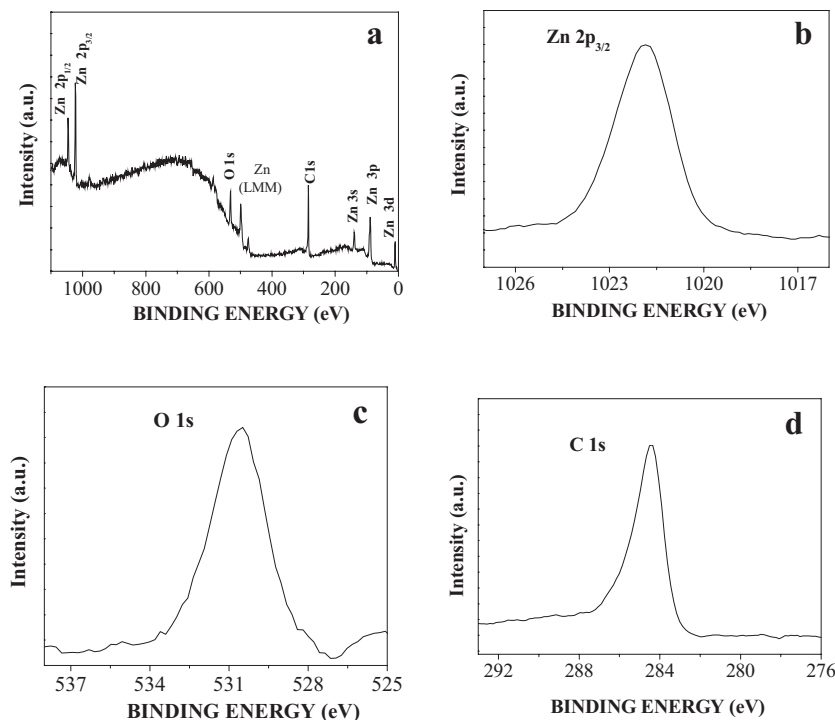


**Figure 3.** a) XPS survey spectrum of the as-prepared products. b) Zn 2p<sub>3/2</sub> spectrum. c) O 1s spectrum. d) C 1s spectrum.

shown in Figure 3d, arises from the graphite-like C–C bond,<sup>[21]</sup> which is similar to that of CNTs prepared by pyrolysis of iron phthalocyanine.<sup>[22]</sup> The absence of oxygen component(s) in the high-resolution XPS C 1s spectrum confirms there is no oxygen bonded to the nanotube structure. Therefore, the XPS data, together with the above microscopy results, unambiguously indicate the formation of ZnO nanoparticles at the tips of aligned CNTs to form an aligned CNT–ZnO heterojunction array.

Similar to many ZnO nanomaterials that possess interesting optoelectronic properties, the CNT–ZnO heterojunctions are attractive for various optoelectronic applications. To assess the optoelectronic properties of the CNT–ZnO heterojunctions, we measured the photoluminescence (PL, excitation wavelength: 325 nm) emission from the as-grown sample after being gently dispersed in water at room temperature. The PL spectrum given in Figure 4a shows a near-band-edge emission at 386 nm (3.20 eV) and a broad blue–green emission band at about 450 nm (2.75 eV). The near-UV emission at 3.20 eV corresponds to the bulk bandgap at 3.35 eV of ZnO and originates from the recombination of free excitons.<sup>[23]</sup> The broad band at approximately 2.75 eV is attributed to the recombination of photogenerated holes with singly ionized oxygen vacancies<sup>[24]</sup> generated possibly by electron transfer from the ZnO nanoparticle of a relatively low work

function (ca. 4.5 eV),<sup>[25]</sup> through the heterojunction, to the aligned CNT tip (ca. 5.0 eV).<sup>[26]</sup> We carried out a control experiment in which the ZnO nanoparticle was deliberately removed from the CNT structure under strong ultrasonication (Model B2510-Mt, 40 kHz) for 1 h. As can be seen in Figure 4b, the same sample solution as for Figure 4a showed a significantly weakened emission band at about 450 nm after ultrasonication (Fig. 4b), due, most likely, to the ultrasonication-induced dissociation of the ZnO nanoparticles from the nanotube heterojunctions (inset Fig. 4b).

Using current-sensing AFM (CSAFM),<sup>[27]</sup> we further studied the electronic characteristics of the aligned CNT–ZnO heterojunctions. Current–voltage (*I*–*V*) curves of the aligned CNT–ZnO heterojunctions were measured by placing a gold-coated conducting AFM tip onto the ZnO nanoparticles with an applied voltage between the conducting AFM tip and Zn substrate (Fig. 5a). The nonlinear *I*–*V* response for the CNT–ZnO heterojunctions (cur-

ve I, Fig. 5b) reveals their semiconducting behavior in the dark. Upon UV illumination (Hg lamp, 4 W and 366 nm), a linear *I*–*V* response with a larger slope was observed (curve II, Fig. 5b). The observed change indicates that the aligned CNT–ZnO heterojunctions assumed a more conductive ohmiclike contact when irradiated with UV light, which is consistent with a decrease in the potential barrier at the junction by the above-bandgap light absorption<sup>[28]</sup> and a photoinduced increase in charge-carrier density.<sup>[29]</sup> The possibility of photoexcitation of charge carriers in the Si AFM tip can be ruled out because there is no significant deviation from the linear *I*–*V* response when *I*–*V* measurements were performed in the dark and under light on the aligned nanotube sample prepared under the same condition without the post-synthesis annealing necessary for the formation of the heterojointed ZnO nanoparticle.

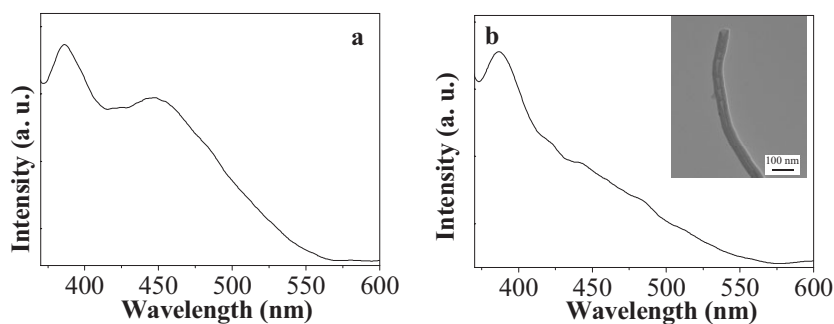


**Figure 4.** Room-temperature PL spectra of an as-grown sample a) after being gently dispersed in water and b) after being strongly ultrasonicated for a prolonged time (i.e., 1 h).

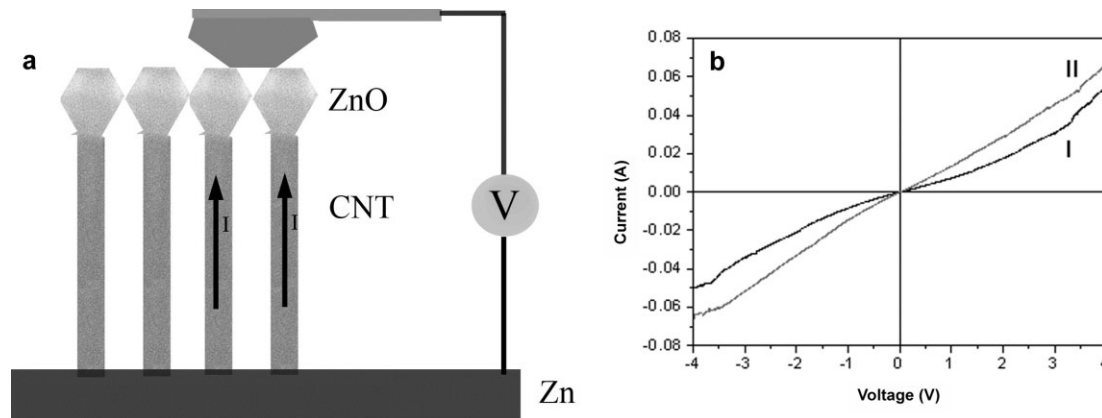


**Figure 5.** a) Schematic representation of the contact configuration for the  $I$ - $V$  measurements. b)  $I$ - $V$  characteristic curves of an aligned CNT-ZnO heterojunction in the dark (curve I) and with UV illumination (curve II). For the sake of clarity, only two of the ZnO nanoparticles are shown to contact with the AFM tip in (a).

In order to exploit the generality of the water-assisted CVD process for producing aligned CNT heterojunctions with ZnO nanostructures of different geometries, we have also systematically varied the growth conditions. It was found that detailed structures of the resultant CNT-ZnO heterojunctions depend strongly on the reaction time. In particular, Figure 6a and b show that the size of the aligned CNT-supported ZnO particles significantly increased with the purging time. Furthermore, the formation of heterojunctions between aligned CNTs and ZnO rods (Fig. 6c) was observed by increasing the Ar flow rate to 600 sccm, while keeping other conditions unchanged. Therefore, the growth conditions play an important role in regulating the size and/or morphology of the ZnO particles in the CNT-ZnO heterojunctions.

In conclusion, we have demonstrated the large-scale synthesis of aligned CNT-ZnO heterojunction arrays by CVD of  $C_2H_2$  on a zinc substrate under Ar and  $H_2$  in the presence of water. SEM and TEM studies revealed intimate contact between the ZnO nanoparticle and aligned CNT. The aligned CNT-ZnO heterojunctions thus prepared were shown to possess interesting optical and optoelectronic properties attractive to a wide range of potential applications. Owing to its simplicity and scalability, the water-assisted growth process developed in the present study could easily be adopted for large-scale, cost-effective production of aligned CNT heterojunctions with ZnO nanostructures of different geometries for various potential applications.

### Experimental

In a typical experiment, the CVD growth of the CNT-ZnO heterojunction arrays was carried out on a zinc foil supported by a quartz glass plate in a tube furnace at  $850^\circ C$  under a combined flow of Ar (300 sccm),  $H_2$  (20 sccm), and  $C_2H_2$  (10 sccm) for 10 min with a portion of the carrier gas passing through a water bubbler. This was then followed by purging the reaction system with a flow of Ar through the water bubbler for 20 min.

SEM imaging was performed on a Hitachi S-4800 field emission microscope. TEM images were taken on a Hitachi H-7600 transmission electron microscope using an accelerating voltage of 120 kV. PL emission spectra ( $\lambda_{EX} = 325$  nm) were recorded on a Perkin Elmer LS 55 luminescence spectrometer while XPS measurements were recorded on a VG Microtech ESCA 2000 using monochromatic Mg K $\alpha$  radiation at a power of 300 W. UV irradiation was carried out with a UL3101 UV lamp (entela).

Received: November 2, 2005  
Final version: March 8, 2006  
Published online: June 8, 2006

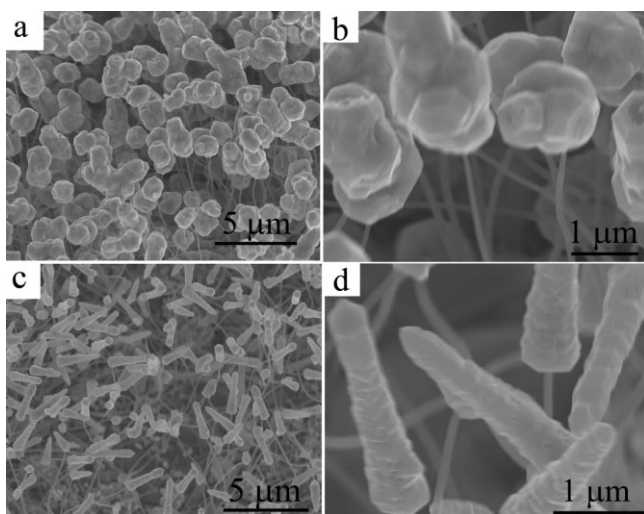


**Figure 6.** a) SEM image of the CNT-ZnO heterojunctions formed by water-assisted growth with an increased purging time of 40 min. b) As for (a), under higher magnification. c) SEM image of the CNT-ZnO rod heterojunctions formed by water-assisted growth with an increased Ar flow rate of 600 sccm. d) As for (c), under higher magnification.

- [1] a) C. Weisbuch, B. Vinter, *Quantum Semiconductor Structures: Fundamentals and Applications*, Academic, San Diego, CA **1991**. b) *Carbon Nanotechnology: Recent Developments in Chemistry, Physics, Materials Science and Device Applications* (Ed: L. Dai), Elsevier, Amsterdam **2006**.

- [2] a) J. Hu, M. Ouyang, P. Yang, C. M. Lieber, *Nature* **1999**, 399, 48. b) M. H. Huang, S. Mao, H. Feick, H. Yan, Y. Wu, H. Kind, E. Weber, R. Russo, P. Yang, *Science* **2001**, 292, 1897.
- [3] a) M. S. Gudiksen, L. J. Lauhon, J. Wang, D. C. Smith, C. M. Lieber, *Nature* **2002**, 415, 617. b) Y. Wu, R. Fan, P. Yang, *Nano Lett.* **2002**, 2, 83.
- [4] a) S. Banerjee, S. S. Wong, *Nano Lett.* **2002**, 2, 195. b) A. Jensen, J. R. Hauptmann, J. Nygard, J. Sadowski, P. E. Lindelof, *Nano Lett.* **2004**, 4, 349. c) H. Kim, W. Sigmund, *Appl. Phys. Lett.* **2002**, 81, 2085.
- [5] F. Qian, Y. Li, S. Gradecak, D. Wang, C. J. Barrelet, C. M. Lieber, *Nano Lett.* **2004**, 4, 1975.
- [6] X. D. Wang, J. H. Song, P. Li, J. H. Ryou, R. D. Dupuis, C. J. Summers, Z. L. Wang, *J. Am. Chem. Soc.* **2005**, 127, 7920.
- [7] J. Du, L. Fu, Z. Liu, B. Han, Z. Li, Y. Liu, Z. Sun, D. Zhu, *J. Phys. Chem. B* **2005**, 109, 12772.
- [8] A. J. Mieszawska, R. Jalilian, G. U. Sumanasekera, F. P. Zamborini, *J. Am. Chem. Soc.* **2005**, 127, 10822.
- [9] a) R. H. Baughman, A. A. Zakhidov, W. A. de Heer, *Science* **2002**, 297, 787. b) P. M. Ajayan, O. Z. Zhou, *Top. Appl. Phys.* **2001**, 80, 391. c) L. Dai, *Intelligent Macromolecules for Smart Devices: From Materials Synthesis to Device Applications*, Springer, New York **2004**.
- [10] See, for example: a) E. C. Greyson, Y. Babayan, T. W. Odom, *Adv. Mater.* **2004**, 16, 1348. b) Y. Zhang, H. Jia, D. Yu, *J. Phys. D* **2004**, 37, 413. c) Y. Li, G. W. Meng, L. D. Zhang, *Appl. Phys. Lett.* **2000**, 76, 2011. d) P. X. Gao, Z. L. Wang, *J. Phys. Chem. B* **2004**, 108, 7534.
- [11] a) J. Goldberger, D. J. Sirbully, M. Law, P. Yang, *J. Phys. Chem. B* **2005**, 109, 9. b) Z. Fan, J. G. Lu, *Appl. Phys. Lett.* **2005**, 86, 032111.
- [12] Q. H. Li, Y. X. Liang, Q. Wan, T. H. Wang, *Appl. Phys. Lett.* **2004**, 85, 6389.
- [13] a) S. H. Jo, D. Banerjee, Z. F. Ren, *Appl. Phys. Lett.* **2004**, 85, 1407. b) Z. L. Wang, X. Y. Kong, Y. Ding, P. Gao, W. L. Hughes, R. Yang, Y. Zhang, *Adv. Funct. Mater.* **2004**, 14, 943. c) J. C. Johnson, H. Yan, P. Yang, R. J. Saykally, *J. Phys. Chem. B* **2003**, 107, 8816. d) P. X. Gao, Z. L. Wang, *J. Appl. Phys.* **2005**, 97, 044304.
- [14] K. Hata, D. N. Futaba, K. Mizuno, T. Namai, M. Yumura, S. Iijima, *Science* **2004**, 306, 1362.
- [15] J. W. Liu, M. W. Shao, X. Y. Chen, W. C. Yu, X. M. Liu, Y. T. Qian, *J. Am. Chem. Soc.* **2003**, 125, 8088.
- [16] D. C. Li, L. M. Dai, S. M. Huang, A. W. H. Mau, Z. L. Wang, *Chem. Phys. Lett.* **2000**, 316, 349.
- [17] Z. Y. Jiang, Z. X. Xie, X. H. Zhang, S. C. Lin, T. Xu, S. Y. Xie, R. B. Huang, L. S. Zheng, *Adv. Mater.* **2004**, 16, 904.
- [18] C. Ducati, I. Alexandrou, M. Chhowalla, G. A. J. Amaratunga, J. Robertson, *J. Appl. Phys.* **2002**, 92, 3299.
- [19] a) P. G. Collins, K. Bradley, M. Ishigami, A. Zettl, *Science* **2000**, 287, 1801. b) L. Fu, Z. Liu, Y. Liu, B. Han, P. Hu, L. Cao, D. Zhu, *Adv. Mater.* **2005**, 17, 217.
- [20] M. Futsuhara, K. Yoshioka, O. Takai, *Thin Solid Films* **1998**, 322, 274.
- [21] J. W. Jang, C. E. Lee, S. C. Lyu, T. J. Lee, C. J. Lee, *Appl. Phys. Lett.* **2004**, 84, 2877.
- [22] a) S. Huang, L. Dai, A. W. H. Mau, *J. Phys. Chem. B* **1999**, 103, 4223. b) Q. Chen, L. Dai, M. Gao, S. Huang, A. Mau, *J. Phys. Chem. B* **2001**, 105, 618.
- [23] a) M. H. Huang, Y. Y. Wu, H. N. Feick, N. Tran, E. Weber, P. D. Yang, *Adv. Mater.* **2001**, 13, 113. b) A. Mitra, R. K. Thareja, *J. Appl. Phys.* **2001**, 89, 2025. c) Y. C. Kong, D. P. Yu, B. Zhang, W. Fang, S. Q. Feng, *Appl. Phys. Lett.* **2001**, 78, 407.
- [24] a) K. Vanheusden, W. L. Warren, C. H. Seager, D. K. Tallant, J. A. Voigt, B. E. Gnade, *J. Appl. Phys.* **1996**, 79, 7993. b) Y. Li, G. W. Meng, L. D. Zhang, F. Phillipp, *Appl. Phys. Lett.* **2000**, 76, 2011.
- [25] K. B. Sundaram, A. Khan, *J. Vac. Sci. Technol. A* **1997**, 15, 428.
- [26] See, for example: a) H. C. Choi, M. Shim, S. Bangsaruntip, H. Dai, *J. Am. Chem. Soc.* **2002**, 124, 9058. b) Z. Xu, X. D. Bai, E. G. Wang, Z. L. Wang, *Appl. Phys. Lett.* **2005**, 87, 163106.
- [27] W. I. Park, G. Yi, J. Kim, S. Park, *Appl. Phys. Lett.* **2003**, 82, 4358.
- [28] K. Keem, H. Kim, G. T. Kim, J. S. Lee, B. Min, K. Cho, M. Y. Sung, S. Kim, *Appl. Phys. Lett.* **2004**, 84, 4376.
- [29] R. D. Sun, A. Nakajima, A. Fujishima, T. Watanabe, K. Hashimoto, *J. Phys. Chem. B* **2001**, 105, 1984.